Letter

Biermann battery effect in laser-excited metals

Ivan Oladyshkin [*]

A.V. Gaponov-Grekhov Institute of Applied Physics of the Russian Academy of Sciences, Nizhny Novgorod, Russia

Interaction of femtosecond optical pulses with solids is accompanied by inhomogeneous electron heating and interband transitions. In the general case it should lead to the excitation of bulk eddy currents due to the misalignment between the gradients of free electrons' pressure and density, similarly to the Biermann battery effect. We consider typical conditions for laser ablation of metals and show that these currents significantly heat electrons and provide convective heat transfer on subpicosecond timescales. Estimated heating depth reaches several hundred nanometers, which coincides with the ablation depth of metals at optical fluences of several J/cm^2.

The excitation of vortex flows by nonparallel gradients of medium pressure and density is a fundamental phenomenon in fluid dynamics. The cross product of these two gradients is a source of fluid vorticity in the hydrodynamic equations. In geophysics, the corresponding value is usually called baroclinity, and it is responsible for many important effects concerning energy and mass transport in the ocean and atmosphere, including the formation of cyclones, mesoscale ocean eddies, and a variety of instabilities.

In plasma physics, an effect of a similar nature is known as the Biermann battery [1]. In most cases it is considered as a mechanism of magnetic field generation in the context of astrophysical problems, in line with Biermann's original idea (see, for example, recent papers [2–4]). The Biermann effect can also play a key role in laser-induced plasma expansion [5–8], where it leads to generation of strong magnetic fields and thus significantly affects dynamics of the medium. Typically, such effects are considered on pico- and nanosecond timescales and for macroscopic plasma expansion distances, when the ions or the crystal lattice already started to move being heated due to collisions with electrons.

However, the prerequisites for the Biermann effect manifestation arise even in purely electronic subsystems of laser-irradiated solids before any heat exchange with the crystal lattice, and so before the start of melting or vaporization processes. The main condition is the existence of different nonuniform spatial distributions of temperature and density of free electrons inside the laser spot (see the schematic picture in Fig. 1). Below we focus on widely studied metals and alloys, where this condition should be fulfilled at least at the subpicosecond timescale.

For example, it was established experimentally that femtosecond laser irradiation of gold leads to electron heating up to the temperature of 5 eV and more than twice the increase of free electron density at incident optical fluences of 3 J/cm^2 [9]. The measured dependencies of electronic

temperature and density on pump intensity are significantly different: while the temperature increases roughly linearly, free electron density remains almost constant at low intensities and then experiences significant increase. It means that their spatial distributions over the irradiated spot are indeed different, and so the temperature and density gradients are misaligned.

The theoretical study of the Biermann effect given in this Letter is motivated by repeatedly confirmed experimental data on femtosecond laser ablation of metals, which still have no generally accepted explanation. First of all, it is the growth of the ablation depth per single laser shot up to ∼0.5–1 micrometer at optical fluences of about 5–10 J/cm^2 [10,11]. The problem is that the electronic thermal conductivity can provide heat transfer from the initially heated skin layer (10–20 nm) only to a depth of about 100 nm in a few picoseconds. By this moment thermal energy is mostly transferred to the crystal lattice and material destruction starts. Moreover, if we take into account a multiple increase of electron collision frequency due to heating [9,12], the estimated maximal depth of heat diffusion occurs to be even smaller.

To resolve this contradiction, the models of femtosecond ablation were proposed which take into account material melting by a shock wave [13–15]. The shock wave is supposed to be excited in the overheated layer and then transfer energy deep into the sample, destroying the crystal lattice. This mechanism allows us to overcome the limitation of diffusive energy transport, however, the underlying molecular dynamics modeling is highly dependent on the mechanisms of electronic thermal conductivity included at the stage of problem formulation [16]. Thus, the energy transport models still remain debatable in the theory of laser ablation.

In this Letter we consider an alternative (or additional) mechanism of the medium heating. We develop a self-consistent theory of eddy currents and magnetic field excitation inside the metal after the femtosecond laser irradiation, by analogy with the Biermann battery effect. We consider the very initial (subpicosecond) stage of the medium dynamics, when the crystal lattice remains relatively cold

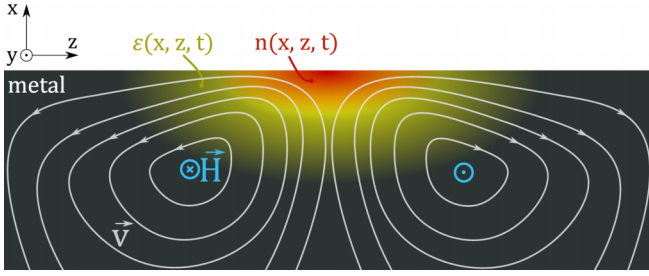[*]Contact author: oladyshkin@ipfran.ru

L140301-1

FIG. 1. Schematic picture of eddy currents excitation after laser irradiation of metal. Red and yellow colors show the areas of increased free electron density and thermal energy, respectively. White lines show free electron velocities.

and only the motion of electrons can be taken into account. Surprisingly, this time period turned out to be sufficient for noticeable increase of electronic temperature caused by the eddy currents.

Further, the introduction of at least two-dimensional (2D) spatial distributions of electronic pressure and density is essentially important, because reducing to 1D geometry obviously eliminates any effects related to vortex motion. For example, a detailed theoretical analysis of the electronic pressure and accompanying electric field influence on femtosecond ablation was carried out in [17]. However, in the paper [17], as in many others, the possibility of eddy current excitation was excluded, since the one-dimensional geometry of the problem was chosen.

Now let us consider free electron gas near the flat metal surface, which was inhomogeneously heated by an ultrashort laser pulse. Below we denote free electron density as $n(x, z)$ and describe degenerate electron gas in terms of the average kinetic (thermal) energy of electron $\varepsilon(x, z)$, which is related to electronic temperature T as $\varepsilon = \frac{3}{5}\varepsilon_F + \frac{\pi^2}{4}\frac{T^2}{\varepsilon_F}$, where ε_F is the Fermi energy. We chose 2D geometry for clarity, assuming that the system is homogeneous along the y axis; see Fig. 1. However, the resulting Eqs. (10)–(13) describing the excitation of magnetic fields and currents are still valid for 3D distributions. In the ideal gas approximation [18], the electronic pressure p can be written as

$$p = \frac{2}{3} n\varepsilon. \tag{1}$$

We use the hydrodynamic model of free electrons and describe their collective motion by the Euler equation, taking into account the pressure gradient ∇p and the self-consisting electric field $\mathbf{E}$:

$$\frac{\partial \mathbf{v}}{\partial t} = -\nu \mathbf{v} - \frac{\nabla p}{nm} - \frac{e\mathbf{E}}{m}, \tag{2}$$

where $\mathbf{v}$ is the electron gas velocity, ∇ is the nabla differential operator, ν is the effective collision frequency, and e and m are the elementary charge and the electron mass, respectively. Note that applicability of the hydrodynamic approach mainly depends on the electron collision frequency, i.e., metal purity and temperature. Because of fast overheating of electrons, preceding melting and ablation, the scattering rate increases strongly [9,12] and the mean free path decreases down to a few nanometers, which is one order smaller than the optical skin-layer depth, so that the Euler equation can be used instead

of the kinetic Boltzmann equation even for highly conductive metals.

The magnetic field action is neglected in Eq. (2) since we limit ourselves to laser fluences of several J/cm^2, when the expected velocities of electrons are comparable to the Fermi velocity, and so are three orders lower than the speed of light. Note that this does not cancel generation of the magnetic field by bulk electric currents. At last, the nonlinear term $(\mathbf{v}\nabla)\mathbf{v}$ is neglected in Eq. (2) in comparison with the electron gas pressure; see the velocity estimations below.

Evolution of the electromagnetic field inside the metal is described by Maxwell's equations:

$$\text{rot } \mathbf{H} = \frac{1}{c}\frac{\partial \mathbf{E}}{\partial t} + \frac{4\pi}{c}\mathbf{j} \tag{3}$$

$$\text{rot } \mathbf{E} = -\frac{1}{c}\frac{\partial \mathbf{H}}{\partial t}, \tag{4}$$

where $\mathbf{H}$ is the magnetic field, $\mathbf{j} = -ne\mathbf{v}$ is the electronic current, and c is the speed of light.

Here we focus on relatively low-frequency processes of current and electromagnetic field propagation inside the metal with the characteristic timescales from several femtoseconds to several picoseconds. Thus, the time derivative in Eq. (2) can be neglected in comparison with the collision frequency, which increases up to $(2-3) \times 10^{15}\,\text{s}^{-1}$ even at moderate pumping fluences. So, from Eq. (2) we find

$$\mathbf{v} \approx -\frac{\nabla p}{\nu nm} - \frac{e\mathbf{E}}{\nu m} \tag{5}$$

and

$$\mathbf{j} \approx \frac{e\nabla p}{\nu m} + \frac{e^2 n\mathbf{E}}{\nu m}. \tag{6}$$

Substitution of Eq. (6) into Eq. (3) gives

$$c \cdot \text{rot } \mathbf{H} = \frac{\partial \mathbf{E}}{\partial t} + \frac{4\pi e\nabla p}{\nu m} + \frac{\omega_p^2 \mathbf{E}}{\nu}, \tag{7}$$

where $\omega_p^2 = \frac{4\pi ne^2}{m}$ is the squared plasma frequency of electrons. In this equation the term $\frac{\partial \mathbf{E}}{\partial t}$ is several orders less than $\frac{\omega_p^2}{\nu}\mathbf{E}$ since the expected timescales of $\mathbf{E}$ variation is at least several femtoseconds, while $\frac{\omega_p^2}{\nu}$ is of the order of 10^{17}–$10^{18}\,\text{s}^{-1}$ in typical metals. Neglecting $\frac{\partial \mathbf{E}}{\partial t}$ in Eq. (7), we find the following relation:

$$\text{rot } \mathbf{H} \cong \frac{4\pi}{c}\mathbf{j} = \frac{4\pi e\nabla p}{\nu mc} + \frac{\omega_p^2 \mathbf{E}}{\nu c}. \tag{8}$$

Expressing electric field $\mathbf{E}$ from Eq. (8) and substituting it into Eq. (4), we obtain

$$-\frac{1}{c}\frac{\partial \mathbf{H}}{\partial t} = \frac{[\nabla n, \nabla p]}{en^2} + \text{rot}\left(\frac{c}{4\pi}\frac{\nu m}{ne^2}\text{rot } \mathbf{H}\right), \tag{9}$$

where square brackets $[\nabla n, \nabla p]$ denote the cross product of two gradients. Let us introduce the magnetic diffusion coefficient $D_H = \nu c^2/\omega_p^2$ and take into account the equation of state (1):

$$\frac{\partial \mathbf{H}}{\partial t} = -\text{rot}(D_H \text{ rot } \mathbf{H}) - \frac{2c}{3en}[\nabla n, \nabla \varepsilon]. \tag{10}$$

This is the equation of diffusion type describing magnetic field excitation and propagation inside the metal. As it was

expected, the source of magnetic field is proportional to the cross product $[\nabla n, \ \nabla\varepsilon]$, which is directed along the y axis in the chosen geometry, so that the magnetic field has only the y component.

In the case of small perturbations, when $n = n_0 + \delta n$, $\nu = \nu_0 + \delta\nu$ and $\delta\nu \ll \nu_0$, $\delta n \ll n_0$, we have $D_H \cong$ const, so that Eq. (10) transforms into the classical diffusion equation, which allows us to get a general idea of the magnetic field propagation inside the metal:

$$\frac{\partial \mathbf{H}}{\partial t} = D_H \ \Delta \ \mathbf{H} - \frac{2c}{3en_0}[\nabla n, \ \nabla\varepsilon]. \qquad (11)$$

Next, calculating the curl of Eq. (10) and taking into account Eq. (8), we find an equation similar to Eq. (10) for the bulk current evolution:

$$\frac{\partial \mathbf{j}}{\partial t} = -\text{rot} \ \{\text{rot}(D_H \ \mathbf{j})\} - \text{rot}\left\{\frac{c^2}{6\pi en}[\nabla n, \ \nabla\varepsilon]\right\}, \qquad (12)$$

which is also transformed into the diffusion equation in the case of small perturbations (when $\delta n \ll n_0$ and $D_H \cong$ const):

$$\frac{\partial \mathbf{j}}{\partial t} = D_H \ \Delta \ \mathbf{j} - \frac{c^2}{6\pi en_0}\text{rot}[\nabla n, \ \nabla\varepsilon]. \qquad (13)$$

Here we should note that under the chosen assumptions the electronic current $\mathbf{j}$ has only an eddy component, and hence zero divergence:

$$\text{div} \ \mathbf{j} = \frac{\partial j_x}{\partial x} + \frac{\partial j_z}{\partial z} = 0, \qquad (14)$$

which directly follows from Eq. (8). It is important that the source of vortex electron motion like $\text{rot}[\nabla n, \ \nabla\varepsilon]$ cannot be shielded by charge separation fields, in contrast to potential sources like the pressure gradient in a homogeneous medium. On the other hand, because of zero divergence, electric currents describing by Eqs. (12) or (13) do not perturb free electron density. However, eddy currents can exist on the background of quasistatic charge separation fields, discussed, for example in the papers [17,19].

Under realistic experimental conditions the characteristic longitudinal scale of the all perturbations l_z is much larger than the transversal scale l_x, since l_z is equal to the laser spot radius, which is at least several microns, and l_x is of the order of optical skin layer, which is 10–20 nm. From the inequality $l_z \gg l_x$ and $\text{div} \ \mathbf{j} \cong 0$ it follows that the z component of the electronic current is much larger than the x component. Thus, from Eqs. (10) and (12) we find

$$\frac{\partial H_y}{\partial t} \cong \frac{\partial}{\partial x}\left(D_H \ \frac{\partial H_y}{\partial x}\right) - \frac{2c}{3en}[\nabla n, \ \nabla\varepsilon]_y, \qquad (15)$$

$$\frac{\partial j_z}{\partial t} \cong \frac{\partial^2 (D_H \ j_z)}{\partial x^2} - \frac{\partial}{\partial x}\left\{\frac{c^2}{6\pi en}[\nabla n, \ \nabla\varepsilon]_y\right\}. \qquad (16)$$

Also, at the impenetrable boundary the normal current is zero, so $j_x = 0$ and $\frac{\partial H_y}{\partial z} = 0$ along the entire surface according to Eq. (8). Because at $z = \pm\infty$ the magnetic field is zero, we obtain $H_y \equiv 0$ along the entire metal surface, so that the magnetic field is localized inside the metal and the electromagnetic energy flux outside the medium is negligible under the chosen assumptions.

For further estimations we mostly use the parameters of overheated gold obtained experimentally in [9,12], and also

take into account the results of first-principles calculations of electronic properties of iron [20] and widespread alloys like stainless steel [20], CuNi, and AuCu [21] in nonequilibrium states (which corresponds to the ablation conditions discussed in the Letter). According to these papers, the listed metals and alloys behave similarly, demonstrating 1.5–2.5 times increase of free electron density after heating up to the temperature of 3–5 eV and negligible growth of electron density at temperatures below ~1 eV.

More specifically, experimental data for gold [9] show that at rather moderate incident laser fluence of 3 J/cm^2 the resulting electronic temperature is ~5 eV (which gives the increase of kinetic energy of Fermi particles $\delta\varepsilon \cong 2.3$ eV), the concentration of free electrons grows from 6×10^{22} cm^{-3} to 15×10^{22} cm^{-3} (so $\delta n = 9 \ \times \ 10^{22}$ cm$^{-3} = 1.5n_0$) and the collision rate increases from 0.13×10^{15} s^{-1} to 4.2×10^{15} s^{-1}. In more recent experiments on ultrafast THz excitation of gold [12] an approximately twice smaller increase of the electronic collision rate was measured, which was mostly attributed to the difference in the irradiated samples' thickness. However, the growth of free electron density was estimated similarly to [9] in the available temperature range up to 1.5 eV.

The thermal diffusivity of electron gas in metals $D = v_F^2/3\nu$ should sufficiently decrease after heating due to the collision rate increase. For the parameters of excited gold given above, D decreases to 2–4 cm^2/s (being of about 50 cm^2/s at room temperature outside the overheated zone), so that the characteristic time of heat diffusion from the overheated optical skin layer $l_{sk} = 12$–15 nm can be estimated as $\tau_D = l_{sk}^2/D \sim 0.5$–1 ps. At the same time, the value of magnetic diffusivity D_H is about 5×10^3 cm^2/s inside the overheated region and one order smaller outside (at room temperature). Thus, the magnetic diffusion is a much faster process than the heat diffusion. Also, the characteristic time of free electron density relaxation is not less than 1 ps. Consequently, the source term $\sim [\nabla n, \ \nabla\varepsilon]_y$ in Eqs. (15) and (16) can be considered as almost constant at timescales smaller than 1 ps, while the magnetic diffusion occurs to be the dominant mechanism of energy transport.

The action of the Birman battery lasts as long as there are significant temperature and density gradients that decrease by electronic heat diffusion, heat exchange with the crystal lattice, and recombination. For many metals these processes have comparable timescales of the order of several picoseconds. During the time τ_D magnetic diffusion spreads magnetic field and eddy currents to the depth of $l_{MD} = \sqrt{D_H \tau_D}$ (about several hundred nanometers), which determines the characteristic heating depth. The longitudinal size of the heated area along the z axis l_z is roughly determined by the laser spot size, or, more precisely, by the distance from the laser spot center to the point where the gradients ∇n and $\nabla\varepsilon$ are most different [for example, where one of $n(z)$ or $\varepsilon(z)$ experiences much sharper decrease than another one].

Let us estimate the generated magnetic field and the electron velocities under the conditions listed above. We calculate these values at the moment of $\tau_D = 1$ ps after the laser pulse action, assuming that the magnetic diffusion spreads magnetic field and electric current to the depth of $l_{MD} = \sqrt{D_H \tau_D} \cong 300$ nm. Estimating the cross product $[\nabla n, \ \nabla\varepsilon]_y$ as $\frac{\delta\varepsilon}{l_z}\frac{\delta n}{l_{sk}}$, we consider the laser beam with the diameter $d = 5$ μm and

peak fluence of 3 J/cm² and take into account experimental data for gold from [9], showing that in this case the electron thermal energy ε has a significantly sharper profile near the beam center than the electron density n. From Eq. (15) we obtain

$$|H_y| \cong \frac{2c\tau_D}{3en} \frac{\delta n}{l_{sk}} \frac{\delta\varepsilon}{l_z} \frac{l_{sk}}{l_{\mathrm{MD}}} \approx 2 \times 10^5 \text{ G.} \qquad (17)$$

The value of current and directed electron velocity inside the metal can be estimated from (8):

$$|v_z| = \left| \frac{j_z}{n_0 e} \right| \approx \frac{1}{n_0 e} \frac{c}{4\pi} \frac{\partial H_y}{\partial x} \approx 6 \times 10^5 \text{ cm/s.} \qquad (18)$$

The presence of current leads to electron heating due to scattering processes. In the general case the absorbed power per unit volume is equal to the scalar product of electric field and bulk current: $P = \mathbf{j}\mathbf{E}$. Out of the overheated region the electronic pressure gradient is negligibly small, so that the electronic current can be described by the Drude model, which formally follows from Eq. (6) with $\nabla p = 0$:

$$j_z = \frac{e^2 n_0 \mathbf{E}}{\nu m}. \qquad (19)$$

Calculating the thermal energy per one electron during the time τ_D as $\Delta\varepsilon = P\tau_D/n$, we find

$$\Delta\varepsilon = \frac{\nu\tau_D m}{e^2 n_0^2} j_z^2 = \nu\tau_D m v_z^2. \qquad (20)$$

This relation has clear physical meaning: During the time τ_D an average electron experiences $\nu\tau_D$ collisions, increasing the thermal energy by $m v_z^2$ each time. For the parameters discussed above we obtain $\Delta\varepsilon \cong 0.1$ eV, and this energy is supposed to be transferred almost completely to the crystal lattice in several picoseconds, during the local heat exchange with electrons, so that the expected temperature increase is of the order of 1000 K, which is sufficient to melt gold, and higher temperatures can be reached within the next 2–3 ps. Note that this ultrafast heating is roughly isochorical, and after that material expansion and shock wave generation take place [22,23]. The additional heating by eddy currents estimated above should significantly modify the initial conditions and further dynamics of these processes.

The experimentally measured ablation rate of gold at the fluence of 3 J/cm² is about 350 nm/shot [10], which seems to be in good agreement with the model of electrons heating by eddy currents. Detailed estimations for other metals are complicated by the lack of experimental data on $\nu(T)$ behavior in the nonequilibrium state, however, we can expect comparable efficiency of Biermann battery at least for several metals and alloys studied in [20,21], since similar growth of free electron density and temperature was predicted for them.

The above calculations were performed for fairly moderate conditions, while in many ablation experiments the optical fluence reaches tens of J/cm². This should cause not only the increase of eddy current magnitude, but also the growth of effective electronic collision frequency and magnetic diffusivity, hence the deeper heating is expected along with higher temperature increase. In this case, of course, the dynamics of the magnetic field and eddy currents cannot be accurately de-scribed by approximate Eqs. (12) and (14) since the diffusion coefficient D_H is strongly inhomogeneous, but Eqs. (17) and (18) should be still valid for the order of magnitude estimations.

Besides the direct electron heating, considered electron motion causes convective heat transport with the heat flux equal to $\nabla\varepsilon\mathbf{v}$. But under the conditions described above, the displacement of electrons along the metal surface Δz during several picoseconds is only of about 10 nm, and even much smaller in the normal direction. So, the effect of convection seems to be negligible.

However, in real experiments the laser pulse absorption profile does not necessarily follow the spatial distribution of optical intensity of the incident pulse. First, local field enhancement on surface roughness can lead to multiple increase of heating and interband transitions' rate at nanometer scales. Second, in laser-solid interaction at damaging conditions the well-known effect of LIPSS (laser-induced periodic surface structures) formation takes place, which is caused by the interference of surface plasmon-polaritons at optical frequency [24]. LIPSS on metals have the spatial period close to the incident wavelength, and they are regularly observed on the periphery of ablation craters. This indicates that the actual absorption profile has a spatial modulation on the optical wavelength scale.

According to the developed theory, subwavelength modulation of free electrons' temperature and density should enhance the effect of local heat convection. In this case convective transport can be several times faster than electronic thermal conductivity. This significantly changes spatiotemporal dynamics of heat transport picture at subpicosecond timescales. Quantitative study of heat dynamics with account of this effect demands detailed numerical modeling which is beyond the scope of this Letter.

The ultrafast Biermann battery effect can also play a role in the case of solid targets (including structured ones) irradiation by much more intense laser pulses [25,26], especially since under such conditions the electron density and temperature distributions are strongly inhomogeneous. However, the developed theory cannot be directly applied to this case, because it does not take into account the ion's motion and kinetic effects beyond the hydrodynamic model.

To sum up, we have considered the role of Biermann battery effect in femtosecond laser ablation of metals. The diffusion-type equation has been derived for the magnetic field and eddy current propagation inside the medium, and it has been shown that magnetic diffusion is much faster than classical electronic thermal conductivity. Basing on the available data for several metals and alloys [9,12,20,21] in the fluence range up to several J/cm², it has been predicted that eddy currents excited inside the metal are sufficiently strong to heat the material at least up to the melting temperature. The convective heat transfer provided by these currents has also been estimated and found to be important on subwavelength spatial scales. Thus, the Biermann effect seems to be an important factor changing free electron dynamics at the very initial stage of laser pulse interaction with metals.

[1] L. Biermann, Uber den Ursprung der Magnetfelder auf Sternen und im interstellaren Raum (mit einem Anhang von A. Schluter), Z. Naturforsch. **5**, 65 (1950).

[2] Y. Ohira, The biermann battery driven by a streaming plasma, Astrophys. J. **911**, 26 (2021).

[3] M. Sherlock and J. J. Bissell, Suppression of the biermann battery and stabilization of the thermomagnetic instability in laser fusion conditions, Phys. Rev. Lett. **124**, 055001 (2020).

[4] R. R. Andreasyan, I. K. Marchevsky, and E. A. Mikhailov, Role of biermann battery mechanism in appearance of magnetic fields in accretion discs, Astron. Rep. **68**, 238 (2024).

[5] J. R. Davies, Nonlocal suppression of Biermann battery magnetic-field generation for arbitrary atomic numbers and magnetization, Phys. Plasmas **30**, 072701 (2023).

[6] J. J. Pilgram, M. B. P. Adams, C. G. Constantin, P. V. Heuer, S. Ghazaryan, M. Kaloyan, R. S. Dorst, D. B. Schaeffer, P. Tzeferacos, and C. Niemann, High repetition rate exploration of the Biermann battery effect in laser produced plasmas over large spatial regions, High Power Laser Sci. Eng. **10**, e13 (2022).

[7] N. Shukla, K. Schoeffler, E. Boella, J. Vieira, R. Fonseca, and L. O. Silva, Interplay between the Weibel instability and the Biermann battery in realistic laser-solid interactions, Phys. Rev. Res. **2**, 023129 (2020).

[8] J. J. Pilgram, C. G. Constantin, H. Zhang, P. Tzeferacos, T. G. Bachmann, L. Rovige, P. V. Heuer, M. B. P. Adams, S. Ghazaryan, M. Kaloyan, R. S. Dorst, M. J.-E Manuel, and C. Niemann, Two-dimensional Thomson scattering measurements of misaligned electron density and temperature gradients and associated Biermann battery produced fields, Phys. Plasmas **31**, 042113 (2024).

[9] C. Fourment, F. Deneuville, D. Descamps, F. Dorchies, S. Petit, O. Peyrusse, B. Holst, and V. Recoules, Experimental determination of temperature-dependent electron-electron collision frequency in isochorically heated warm dense gold, Phys. Rev. B **89**, 161110(R) (2014).

[10] M. E. Shaheen, J. E. Gagnon, and B. J. Fryer, Femtosecond laser ablation behavior of gold, crystalline silicon, and fused silica: A comparative study, Laser Phys. **24**, 106102 (2014).

[11] J. Byskov-Nielsen, J.-M. Savolainen, M. S. Christensen, and P. Balling, Ultra-short pulse laser ablation of metals: Threshold fluence, incubation coefficient and ablation rates, Appl. Phys. A **101**, 97 (2010).

[12] Z. Chen *et al.*, Ultrafast multi-cycle terahertz measurements of the electrical conductivity in strongly excited solids, Nat. Commun. **12**, 1638 (2021).

[13] Z. Zhang and G. Gogos, Theory of shock wave propagation during laser ablation, Phys. Rev. B **69**, 235403 (2004).

[14] V. A. Khokhlov *et al.*, Melting of titanium by a shock wave generated by an intense femtosecond laser pulse, JETP Lett. **115**, 523 (2022).

[15] V. V. Shepelev, Yu. V. Petrov, N. A. Inogamov, V. V. Zhakhovsky, E. A. Perov, and S. V. Fortova, Attenuation and inflection of initially planar shock wave generated by femtosecond laser pulse, Opt. Laser Technol. **152**, 108100 (2022).

[16] M. E. Povarnitsyn, N. E. Andreev, E. M. Apfelbaum, T. E. Itina, K. V. Khishchenko, O. F. Kostenko, P. R. Levashov, and M. E. Veysman, A wide-range model for simulation of pump-probe experiments with metals, Appl. Surf. Sci. **258**, 9480 (2012).

[17] V. I. Mazhukin, M. M. Demin, A. V. Shapranov, and A. V. Mazhukin, Role of electron pressure in the problem of femtosecond laser action on metals, Appl. Surf. Sci. **530**, 147227 (2020).

[18] L. P. Pitaevskii and E. M. Lifshitz, *Physical Kinetics* (Elsevier, Amsterdam, 2012).

[19] I. V. Oladyshkin, D. A. Fadeev, and V. A. Mironov, Thermal mechanism of laser induced THz generation from a metal surface, J. Opt. **17**, 075502 (2015).

[20] E. Bevillon, J.-P. Colombier, A. Dutta, and R. Stoian, Ab Initio nonequilibrium thermodynamic and transport properties of ultrafast laser irradiated 316L stainless steel, J. Phys. Chem. C **119**, 11438 (2015).

[21] D. Iabbaden, A. Tsaturyan, J.-M. Raulot, and J.-P. Colombier, Nonequilibrium electronic properties and stability consequences in metallic crystalline binary alloys under ultrafast laser excitation, J. Alloys Compd. **1010**, 177175 (2025).

[22] M. E. Povarnitsyn, T. E. Itina, M. Sentis, K. V. Khishchenko, and P. R. Levashov, Material decomposition mechanisms in femtosecond laser interactions with metals, Phys. Rev. B **75**, 235414 (2007).

[23] M. E. Povarnitsyn, K. V. Khishchenko, and P. R. Levashov, Phase transitions in femtosecond laser ablation, Appl. Surf. Sci. **255**, 5120 (2009).

[24] J. Bonse and S. Gräf, Maxwell meets Marangoni – a review of theories on laser-induced periodic surface structures, Laser Photonics Rev. **14**, 2000215 (2020).

[25] A. Laso Garcia *et al.*, Cylindrical compression of thin wires by irradiation with a Joule-class short-pulse laser, Nat. Commun. **15**, 7896 (2024).

[26] L. Yang *et al.*, Dynamic convergent shock compression initiated by return current in high-intensity laser–solid interactions, Matter Radiat. Extremes **9**, 047204 (2024).